Int. J Heat Mass Transfer Vol 20, pp 113–122 Pergamon Press 1977. Printed in Great Britain

NONLINEAR TWO DIMENSIONAL BÉNARD CONVECTION WITH SORET EFFECT: FREE BOUNDARIES

J. K. PLATTEN and G. CHAVEPEYER
Department of Thermodynamics, University of Mons, 7000—Mons, Belgium

(*Received* 23 *February* 1975 *and in revised form* 5 *July* 1976)

Abstract—This paper describes a numerical analysis of finite amplitude convection in a two-component fluid taking into account thermal diffusion. The present problem is equivalent to the case of thermohaline convection with an additional term in the diffusion equation representing the Soret effect. The nonlinear equations with free boundary conditions are integrated numerically. Near the neutral stability curve, the results of the linear stability theory are recovered for small perturbations, as it should be, but finite amplitude convection is the main subject of this paper. Recent published experimental data seem to indicate that new physical phenomena are caused by the Soret effect: essentially an hysteresis loop was found in Schmidt–Milverton plots and oscillations were also reported when a two component system is heated from below. This paper is an attempt to describe theoretically the experimental facts. During the numerical integration of the nonlinear equations, we have found, in many cases, transient oscillations in the Nusselt number. These oscillations are induced by the Soret effect, and the frequency, or the amplitude can be related to the thermal diffusion coefficient. We give also in this paper an evidence of finite amplitude convection, below the critical Rayleigh number (subcritical instabilities) and thus an hysteresis loop can be described in the Nusselt–Rayleigh number plane.

NOMENCLATURE

$A_{p,q}$, $B_{p,q}$, $C_{p,q}$, Fourier coefficients;
D, isothermal diffusion coefficient;
D', thermal diffusion coefficient;
d, depth of the liquid layer;
g, acceleration due to gravity;
L, length of the cell;
N_i, mass fraction of component i;
N_i^*, initial mass fraction of component i;
Nu, Nusselt number;
n, perturbation of N;
Pr, Prandtl number;
Ra, Rayleigh number;
R_{Th}, Rayleigh number for the concentration field;
Sc, Schmidt number;
$\mathscr{S}$, Soret number;
T, temperature;
t, time;
T, period of oscillations;
x_i, space coordinate.

Greek symbols

α, thermal expansion coefficient;
γ, $\rho^{-1}(\partial\rho/\partial N)_T$;
κ, thermal diffusivity;
ν, kinematic viscosity;
ρ, density;
ϑ, temperature perturbation;
ψ, stream function.

INTRODUCTION

MEASUREMENTS of thermal diffusion coefficient (also called the Soret coefficient; ([1] p. 273) are usually conducted with a liquid layer bounded by two rigid boundaries and heated from above, and thus the system is supposed to be in a state of mechanical equilibrium (convection-free). By monitoring concentration changes, it is possible to deduce the Soret coefficient. But measurements obtained by slightly different methods (e.g. a Clausius column or a flow-cell method) did not always agree with the values given by the direct method. It is now well known [2] that an instability of the system is responsible for the discrepancy between the data reported in the literature. On the other hand, it was suggested by Prof. I. Prigogine that measurements of Soret coefficients could be performed by heating the system from below. Indeed, let us suppose that due to the Soret effect, the denser component migrates towards the bottom (hot boundary): this is thus a stabilizing effect and the increase of the critical temperature gradient necessary to induce convection should be related to the value of the Soret coefficient. Experimental research in this direction was initiated by Legros and coworkers [3–5], and was recently used by Caldwell [6] in order to determine Soret coefficients in electrolyte solutions.

Thus the Rayleigh–Bénard convection in a two-component system has received this last decade a great deal of attention. The first type of problems investigated in this field is the so-called "thermohaline convection". In the second type of problems, a two-component system, *initially homogeneous*, is subjected to an adverse temperature gradient. Thermal diffusion takes place and a mass fraction distribution is established in the liquid layer. This mass fraction distribution has a profound influence on the Bénard convection. Of special interest is the possible application of this type of problem to oceanography (study of convection currents in liquids stratified both by temperature and salt, with a coupling between the two diffusion phenomena) or to crystal growth (especially alloys), from the melt, where temperature gradients in a binary system, could

inhibit or induce prematurely convection, with or without oscillations.

The works of Veronis, Sani, Nield, Shirtcliffe, Baines, Gill, Turner, Hurle, Jakeman, Bdzil, Frisch, Stern and many others are reviewed and discussed in a recent paper [7], where all the suitable references can be found. We want in this paper to report results of a numerical study of finite amplitude convection, coupled with the Soret effect in the case of free boundaries.

Section 2 is devoted to the derivation of the nonlinear equations and to a summary of the results of the linear theory. The numerical results are given in Section 3. An hysteresis loop is described in Section 4. A comparison with the few existing experimental data is given in Section 5.

2. THE NONLINEAR EQUATIONS

In writing the nonlinear equations, we have adopted the following assumptions, essentially the same as in the linear theory:

1. A Boussinesq fluid.
2. The Dufour effect is neglected. This is of course a quite reasonable assumption for liquid mixtures, but becomes inadequate for gases (for more details, see [1] p. 279).
3. The barycentric reference frame is used.

These conservation equations are in a dimensionless form (Z is the vertical and x the horizontal coordinate):

(a) Conservation of mass

$$Sc\frac{\partial N_1}{\partial t} = Sc\frac{\partial(\psi, N_1)}{\partial(x, z)} + \nabla^2 N_1 + \mathscr{S}\nabla^2 T \tag{1}$$

(b) Conservation of momentum (ψ: stream function)

$$Pr\frac{\partial}{\partial t}\nabla^2\psi = Pr\frac{\partial(\psi, \nabla^2\psi)}{\partial(x, z)} - Ra\frac{\partial T}{\partial x} + R_{Th}\frac{\partial N_1}{\partial x} + Pr\nabla^2(\nabla^2\psi) \tag{2}$$

(c) Conservation of energy

$$Pr\frac{\partial T}{\partial t} = Pr\frac{\partial(\psi, T)}{\partial(z, x)} + \nabla^2 T. \tag{3}$$

The Bénard problem including thermal diffusion is characterized by 5 dimensionless parameters. The notation is that adopted in previous papers by Legros and Platten (e.g. [8]).

1. The usual Rayleigh number $Ra = g\alpha\Delta T d^3/\kappa\nu$.
2. The thermal diffusion Rayleigh number $R_{Th} = g\gamma N_1^* d^3/\kappa\nu$ where $\gamma = \rho^{-1}(\partial\rho/\partial N_1)_T$.
   N_1^*: initial mass fraction of component 1 (the more dense).
3. The Soret number $\mathscr{S} = (D'/D)/\Delta T$.
   D: isothermal diffusion coefficient.
   D': thermal diffusion coefficient.
4. The Prandtl number $Pr = \nu/\kappa$.
5. The Schmidt number $Sc = \nu/D$.

The contribution of the conduction regime (linear concentration and temperature profiles) is usually subtracted from equations (1)–(3).

Thus we write

$$\begin{aligned} \psi(x, z, t) &= 0 + \psi(x, z, t) \\ N_1(x, z, t) &= \overline{N_1}(z) + n(x, z, t) \\ T(x, z, t) &= \overline{T}(z) + \vartheta(x, z, t) \end{aligned} \tag{4}$$

with $\overline{T}(z) = 1 - z$ and $\overline{N_1}(z) = 1 + \mathscr{S}(z - 1/2)$.

The final equations to be integrated are

$$Sc\frac{\partial n}{\partial t} = Sc\left[\frac{\partial(\psi, n)}{\partial(x, z)} + \frac{\partial\psi}{\partial x}\cdot\mathscr{S}\right] + \nabla^2 n + \mathscr{S}\nabla^2\vartheta \tag{5}$$

$$Pr\frac{\partial}{\partial t}\nabla^2\psi = Pr\frac{\partial(\psi, \nabla^2\psi)}{\partial(x, z)} - Ra\frac{\partial\vartheta}{\partial x} + R_{Th}\frac{\partial n}{\partial x} + Pr\nabla^2(\nabla^2\psi) \tag{6}$$

$$Pr\frac{\partial\vartheta}{\partial t} = Pr\left[\frac{\partial(\psi, \vartheta)}{\partial(x, z)} - \frac{\partial\psi}{\partial x}\right] + \nabla^2\vartheta \tag{7}$$

together with the free boundary conditions

$$\begin{aligned} &\vartheta = 0 \text{ for } z = 0 \text{ and } z = 1 \\ &\frac{\partial\vartheta}{\partial x} = 0 \text{ for } x = 0 \text{ and } x = L/d \\ &\frac{\partial\psi}{\partial x} = \frac{\partial^2}{\partial z^2}\left(\frac{\partial\psi}{\partial x}\right) = 0 \text{ for } z = 0 \text{ and } z = 1 \\ &\frac{\partial\psi}{\partial z} = \frac{\partial^2}{\partial x^2}\left(\frac{\partial\psi}{\partial z}\right) = 0 \text{ for } x = 0 \text{ and } x = L/d \\ &n = \frac{\partial^2 n}{\partial z^2} = 0 \text{ for } z = 0 \text{ and } z = 1 \\ &\frac{\partial n}{\partial x} = 0 \text{ for } x = 0 \text{ and } x = L/d. \end{aligned} \tag{8}$$

It was found that for $\mathscr{S} > 0$, the principle of exchange of stabilities is valid and the critical Rayleigh number is given by

$$Ra_{(ex)}^{(crit)} = \frac{27\pi^4}{4} - R_{Th}\cdot\mathscr{S}\cdot\frac{Pr + Sc}{Pr}. \tag{9}$$

For $\mathscr{S} < 0$, two cases are possible:

(i) exchange of stabilities for small $|\mathscr{S}|$ and equation (9) is still valid

(ii) overstability for

$$|\mathscr{S}| > \frac{27\pi^4}{4}\frac{Pr(Pr+1)}{R_{Th}\cdot Sc^2}.$$

In that case, the critical Rayleigh number increases more slowly and is given by

$$Ra_{(over)}^{(crit)} = \frac{27\pi^4}{4}\cdot\frac{(1+Sc)(Sc+Pr)}{Sc^2} - R_{Th}\cdot\mathscr{S}\cdot\left(\frac{Pr}{Pr+1}\right). \tag{10}$$

Finally the dimensionless frequency is also known.

$$\sigma_I = \left[\frac{-R_{Th}\cdot\mathscr{S}}{3Pr(Pr+1)} - \frac{9\pi^4}{4Sc^2}\right]^{1/2}. \tag{11}$$

Typical values of the period is O (10^2 s) for a liquid depth of O (1 mm). For more details, see [9].

The method of solution of equations (5)–(7) here adopted, is the method proposed in earlier work by Veronis [10–12] and by Foster [13]. The stream function ψ, the temperature ϑ and mass fraction n are ex-

panded in Fourier components with time dependent coefficients. By substitution of this representation into the nonlinear equations, we get in an absolutely standard manner the time evolution of each Fourier coefficient.

The purely algebraic part is rather long, and can be found elsewhere [21].

The differential equations describing the time evolution of the Fourier coefficient, are integrated numerically, given a suitable set of initial conditions. This is performed by standard numerical methods (Runge–Kutta–Hammings). At each time step, the Nusselt number Nu is computed. The Nusselt number is defined as the ratio of the vertical heat flux to the conductive heat flux. In fact we use a horizontally averaged Nusselt number, and computed at the lower boundary since the heat flux may vary with Z for time-dependent motions. However we can use this definition to describe finite amplitude motions and to deduce the period of the oscillations. Thus

$$Nu = 1 - \pi \sum_{q=1}^{Q} q B_{0,q} \tag{12}$$

if we use for ϑ the following expansion

$$\vartheta = \sum_{p=0}^{P} \sum_{q=1}^{Q} B_{p,q}(t) \cos\left(p\pi \frac{d}{L} x\right) \sin(q\pi z). \tag{13}$$

The numerical results to be presented, are obtained with a truncated representation.

We have used three representations:

(i) $P = Q = 2$; (ii) $P = Q = 4$; (iii) $P = Q = 6$.

The number of Fourier coefficients to be used in order to obtain accurate Nusselt numbers has been discussed previously [10–12]. The results which are physically relevant, are those which do not change in any significant way when the truncation level in the Fourier representation is increased. It was verified in a few numerical experiments that the difference in the numerical results concerning the mean value of the Nusselt number never exceeds 1% between the representation "$P = Q = 4$" and "$P = Q = 6$". This is due to the fact that we are interested in small Rayleigh numbers, in low intensity convection (usually $Ra < 2Ra^{crit}$) and thus the few first modes are sufficient. Some results presented in this paper are obtained with $P = Q = 2$, mainly in order to reduce the computer time. This produces a maximum error of 15% on the Nusselt number. However, the aim of this paper is only to provide a qualitative study of oscillations and of the hysteresis loop. Moreover, accurate Nusselt numbers for the case of two free boundaries, cannot be checked by experiment.

Before proceeding with the numerical integration of the differential equations for the Fourier coefficients of the stream function ψ, the temperature ϑ and the mass fraction n (called respectively $A_{p,q}$, $B_{p,q}$ and $C_{p,q}$), a suitable set of initial conditions must be specified. The values

$$A_{p,q} = B_{p,q} = C_{p,q} = 0 \qquad \forall p, q$$

correspond to the state of rest. We want, in general, to perturb slightly the state of rest and to follow the time evolution of the perturbations. Therefore we have generally adopted the following initial conditions

$$A_{p,q} = C_{p,q} = 0 \quad \forall p, q$$
$$\text{and} \quad |B_{p,q}| = 10^{-6} \text{ for } p = 0, 1 \text{ and } q = 1, 2$$

i.e. an "infinitesimal" perturbation. The contribution of this initial perturbation to the Nusselt number (initially equal to 1) is less than 10^{-6}! The parameters Pr, R_{Th} and Sc were kept constant and equal to $Pr = 10$; $Sc = 1000$; $R_{Th} = 40000$. These values are of the same order of magnitude as for water–alcohol systems (e.g. the system 90 wt% water −10 wt% isopropanol studied experimentally by the authors [9]). Finally, we have adopted $L/d = 1.4$, i.e. one half of the critical wavelength. We are thus studying above the critical point one half of a Bénard cell having the same size as at the critical point. Any other ratio length to depth gives a lower Nusselt number. We have verified that the results of Foster [13] concerning the effect of the ratio L/d are unaffected by thermal diffusion.

The two remaining parameters Ra and $\mathscr{S}$ are varied in the subsequent numerical experiments.

Finally, we would like to mention that all the calculations were done in double precision on a B5500 computer or on a CDC 6400.

3. NUMERICAL RESULTS

(a) *Results near the neutral stability curve for $\mathscr{S} < 0$*

For $\mathscr{S} = -5 \cdot 10^{-3}$, the critical Rayleigh number is from equation (10): $Ra^{(crit)}_{(over)} = 846.557$. The first run was performed with $Ra = 860$, i.e. near the neutral stability curve. At each time step ($\Delta t = 10^{-2}$) all the Fourier coefficients and the Nusselt number are computed.

As predicted by the linear theory the Nusselt number increases with time ($Ra > Ra^{crit} \Rightarrow$ instability) and oscillations of increasing amplitude are observed (overstability). The following experiments were made near the neutral stability curve, namely

1. $\mathscr{S} = -10^{-5}$ $Ra = 660$
2. $\mathscr{S} = -10^{-5}$ $Ra = 670$ $\rightarrow (Ra^{crit}_{over} = 665.1)$
3. $\mathscr{S} = -10^{-4}$ $Ra = 660$
4. $\mathscr{S} = -10^{-4}$ $Ra = 675$ $\rightarrow (Ra^{crit}_{over} = 668.375)$
5. $\mathscr{S} = -10^{-3}$ $Ra = 695$
6. $\mathscr{S} = -10^{-3}$ $Ra = 705$ $\rightarrow (Ra^{crit}_{over} = 701.103)$
7. $\mathscr{S} = -5 \cdot 10^{-3}$ $Ra = 860$ $\rightarrow (Ra^{crit}_{over} = 846.557)$.

In runs (1), (3) and (5), i.e. below the critical point, the initial small perturbations die out. On the contrary, in runs (2), (4), (6) and (7), i.e. above the critical point, the initial perturbations are amplified; the Nusselt number grows with time and oscillates. The general behaviour in view of the seven runs, is indeed the right one. Moreover, the dimensionless period of the oscillations of the Nusselt number, can be deduced from the computer output. For example, for run (7) we have found for the period $T = 4.015$. In fact the period of oscillations of the stream function at each point is twice

the period of oscillations of Nu. This can be easily followed in the numerical results. The velocity components change sign with time. The minimum in ψ (a negative value, thus a maximum in $|\psi|$) as well as a maximum in ψ (positive), correspond both to a maximum in the Nusselt number and this is of course easily understood. When ψ passes through the value zero the Nusselt number is nearly equal to unity. Thus from the computer output the period of oscillations of ψ is $\mathbf{T} = 8.03$. From equation (11), we find $\mathbf{T} = 2\pi/\sigma_I = 8.07$ and this is a surprisingly good agreement. Table 1 summarizes the period of oscillations of the Nusselt number

Table 1

$\mathscr{S}$	$\mathbf{T}_{Nu}$	$\mathbf{T}_{\psi}$	Equation (11)
-10^{-5}	108.5	217	180.47
-10^{-4}	28.96	57.92	57.07
-10^{-3}	8.97	17.94	18.05
$-5\cdot10^{-3}$	4.015	8.03	8.07

$\mathbf{T}_{Nu}$ (column 2), of ψ, called $\mathbf{T}_{\psi}$ (column 3) and the value predicted by the linear theory (equation 11). The poor agreement at $\mathscr{S} = -10^{-5}$ is due to the fact that for $0 < t < 250$ we have only three maxima in Nu to determine $\mathbf{T}_{Nu}$ ($t = 250$ is the final integration time with a time step of 10^{-2}).

We conclude thus that the linear stability theory is verified in these nonlinear computer experiments.

The numerical results of this section [Section 3(a)] were obtained with $P = Q = 2$, and are near the neutral stability curve in complete agreement with the linear theory and there is thus no need to improve any more these results using a higher representation.

(b) *Results at* $\mathscr{S} = -10^{-2}$ *and* $Ra = 2630$ *or* 1800

The critical Rayleigh number is 1028.35 and the numerical results should not be compared with the linear theory. For the same initial perturbation, Fig. 1 shows the Nusselt number vs time for $0 \leqslant t \leqslant 40$.

There is a very rapid growth of the Nusselt number, but as soon as the Nusselt number has reached its final mean value, oscillations start around this mean value. The period of oscillations is $\simeq 1.5$–1.6 and cannot be compared with the value deduced from the linear theory ($\mathbf{T} = 5.7$). This is of course obvious, far from the critical point.

In contradistinction with the numerical results of Section 3(a) the stream function ψ oscillates with exactly the same period as Nu, and never changes sign. There is thus no reversal of the velocity components and thus the minimum of Nu during an oscillation is never 1. The final *mean* value of Nu is 3.04, i.e. exactly the same value that we have obtained in a preliminary run ($\mathscr{S} = 0$), for the usual Bénard problem, at the same Rayleigh number, where of course no oscillations are seen. This is not surprising as we know that, for the case of two free boundaries, the number of convective cells is not affected by thermal diffusion.

Beats are observed. It seems that two frequencies

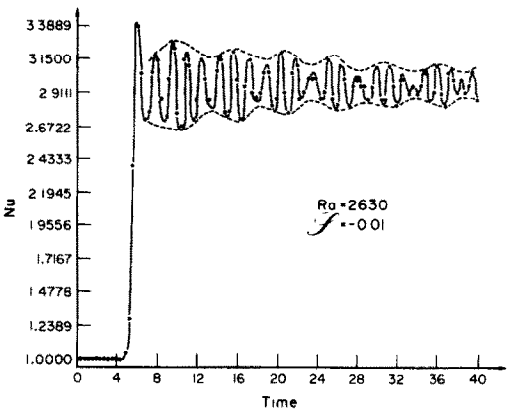

FIG. 1. Time variation of the Nusselt number; Ra:2630; Soret number is -10^{-2}. In all the subsequent figures of this type, the points (●) correspond to the computer output. Solid and dotted lines are added by the authors. The values of the Nusselt number on the y-axis are due to the fact that the computer takes the minimum and the maximum value of Nu, and divides this interval in ten parts. The figures are thus drawn by the computer.

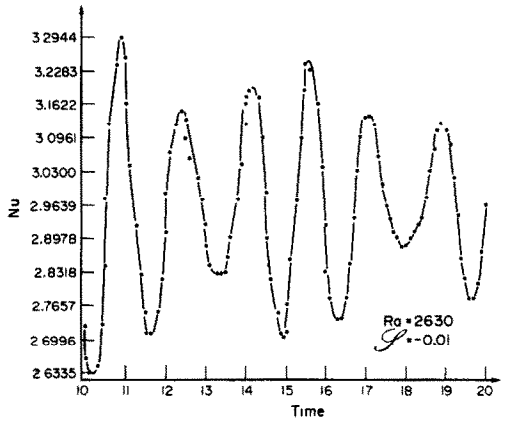

FIG. 2. Time variation of the Nusselt number ($10 \leqslant t \leqslant 20$); $Ra = 2630$; $\mathscr{S} = -10^{-2}$.

are present. This is more evident on Fig. 2 where the time scale is extended and the number of points twice that of Fig. 1 for the same time interval. In fact, with 56 Fourier coefficients, 4 coefficients contribute to the value of Nu (B_{01}, B_{02}, B_{03}, B_{04}). Two of them are less amplified (B_{01} and B_{03}) and contribute for a total amount of less than 0.1% to the Nusselt number. In order to save processor time, the non contributing coefficients are usually neglected and put equal to zero in the integration process. The two remaining coefficients (B_{02} and B_{04}) do not oscillate each with a single but different frequency, as we first expected but beats are observed in each Fourier coefficient. At $Ra = 1800$, the Nusselt number (approximated by $Nu = 1 - 2\cdot\pi\cdot B_{02} - 4\cdot\pi\cdot B_{04}$), presents small irregularities at $t \simeq 32$, $t \simeq 37.5$ and $t \simeq 43.5$ (see arrows in Fig. 3) corresponding to a progressive growth of a new peak, fully developed for large time. For the next higher approximation ($P = Q = 6$), among the 120 coefficients, 60 are not amplified to a significant level ($p+q$ odd)

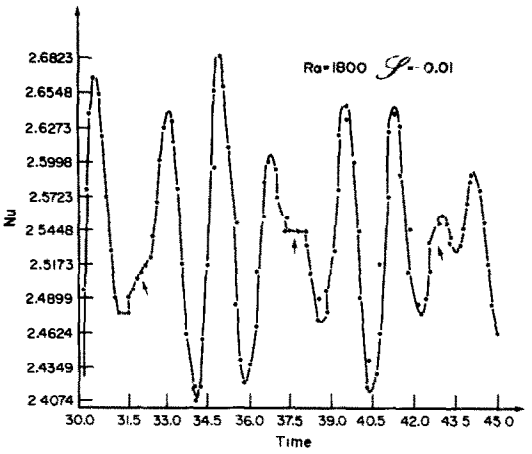

FIG. 3. Time variation of the Nusselt number ($30 \leqslant t \leqslant 45$); $Ra = 1800$; $\mathscr{S} = -10^{-2}$.

and are neglected. Three Fourier coefficients contribute to the Nusselt number (B_{02}, B_{04} and B_{06}). The behaviour of $Nu(t)$ is qualitatively the same as in Figs. 1–3, and no new features are observed. Thus we believe really that only two frequencies are present. At the critical point however, only one frequency is present. We believe that the two frequencies observed at $Ra = 1800$, could be called "the beginning of turbulence".

(c) *Results at* $\mathscr{S} = -10^{-2}$ *and* $Ra = 1100$

This experiment was chosen because the behaviour of Nu for "small" time ($0 \leqslant t \leqslant 160$) is quite similar to that described in Section 3(a). At $t \simeq 200$, the nonlinear terms become sufficiently important and the behaviour of Nu changes radically.

Figure 4 shows $Nu(t)$ for $20 \leqslant t \leqslant 40$. As predicted

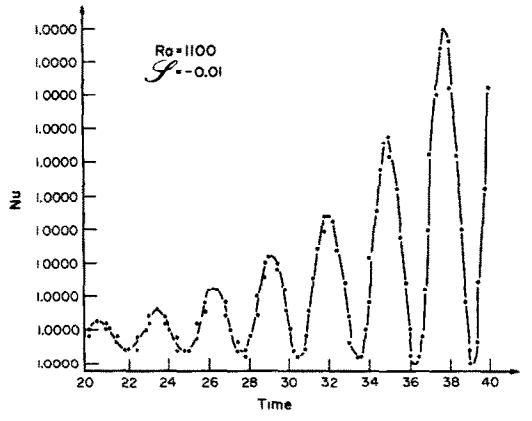

FIG. 4. Growth of the initial perturbation in the Nusselt number. $Ra = 1100$; $\mathscr{S} = -10^{-2}$.

by the linear theory, instability arises as oscillations of increasing amplitude. The behaviour of Nu does not change for $t \leqslant 160$. Figure 4 is reproduced for $40 \leqslant t \leqslant 60$, $60 \leqslant t \leqslant 80$, etc.... The maximum value of Nu during each time interval increases and is given in Table 2. In view of the smallness of the maximum

Table 2

Time interval	Max. of Nu
$20 \leqslant t \leqslant 40$	1.000 000 001
$40 \leqslant t \leqslant 60$	1.000 000 024
$60 \leqslant t \leqslant 80$	1.000 000 429
$80 \leqslant t \leqslant 100$	1.000 007 804
$100 \leqslant t \leqslant 120$	1.000 142 033
$120 \leqslant t \leqslant 140$	1.002 569 826
$140 \leqslant t \leqslant 160$	1.042 148 639

value of Nu for $t < 100$, the ordinate scale in Fig. 4 is correctly labelled, the variation of Nu being less than 0.0001!

The period of oscillations of Nu is $\mathbf{T} = 2.84$. Exactly as in Section 3(a), ψ changes sign and oscillates with a period twice that of Nu. Thus $\mathbf{T}_\psi = 5.68$. The period calculated from equation (11) is $\mathbf{T}_\psi = 5.71$, thus once more a surprisingly good agreement. The period does not change for $t \leqslant 160$. For $t \geqslant 160$, the nonlinear terms become more and more important; the mean value of Nu does no longer increase exponentially as in Fig. 4, but much more slowly. At the same time, there is a modification in the period of the oscillations. For $250 \leqslant t \leqslant 260$, the minimum value of Nu is always of the order of 1, and exactly as for $0 \leqslant t \leqslant 160$, ψ changes sign and passes through the value 0 when $Nu = 1$. The Nusselt number is equal to 1 for the last time at $t \simeq 258$. Indeed, during the next oscillation, Nu drops only to a value close to 1.16 (at $t \simeq 261.7$). The next minima (at $t = 265.8$ and 269.6) are at higher values. At the same time, the successive maxima in Nu decrease. This is shown on Fig. 5.

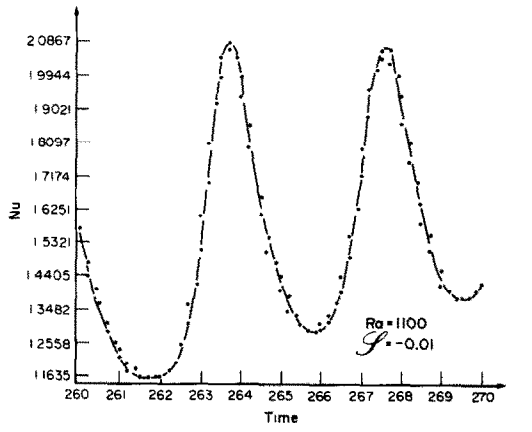

FIG. 5. Time variation of the Nusselt number ($260 \leqslant t \leqslant 270$); $Ra = 1100$; $\mathscr{S} = -10^{-2}$.

What is now remarkable, is that the stream function does no longer change sign and now oscillates with the same period as the Nusselt number. There is thus an acceleration of the convective motion, followed by a retardation of this motion, but without inversion of the velocity components. For $t > 270$, the amplitude of the oscillations decreases. At $t \to \infty$ the amplitude of the oscillations reaches zero.

For this Ra number, there exists thus three domains:

(i) $t < 160$: according to the linear theory, instability arises as oscillations of increasing amplitude and the period is correctly predicted by equation (11). The stream function changes sign and Nu oscillates between 1 and a value greater than 1.

(ii) $160 < t < 260$: the nonlinear terms become important, implying a modification of the period of oscillations. The stream function still changes sign.

(iii) $t > 260$: the Nusselt number oscillates between two values greater than 1 and there is no longer a change of sign in the stream function. The amplitude of the oscillations decreases continuously and the period cannot be predicted by equation (11), i.e. by the linear theory.

(d) *Results for positive Soret numbers at* $Ra \simeq Ra^{crit}$

Different runs were performed *near* the neutral stability curve. In contradistinction with the case $\mathscr{S} < 0$, the growth of the initial perturbation above the critical point, is monotonous in accordance with the fact that, from the linear theory, the principle of stability is valid.

(e) *Results at* $\mathscr{S} = +1.2 \times 10^{-4}$ *and* $Ra \gg Ra^{crit}_{(ex)}$

The first run is performed with $R = 850$. The critical Rayleigh number is 172.7 and thus $Ra \simeq 5 \times Ra^{crit}_{(ex)}$. For $0 < t < 34$ we observe a monotonous growth of the initial perturbation according to the linear theory. As soon as the nonlinear terms are dominant ($t > 34$) oscillations start. This was unexpected but there is no reason to extrapolate the principle of exchange of stability (no oscillations in the initial growth) to the final finite amplitude motion. The period of oscillation is, in reduced units 4.7 and cannot be compared with the value deduced from the linear theory.

The second run is performed with $R = 2630 \simeq 15 \times Ra^{crit}_{(ex)}$ and shows the same behaviour. This is reproduced on Fig. 6 for $0 < t < 10$. It seems that Nu is a

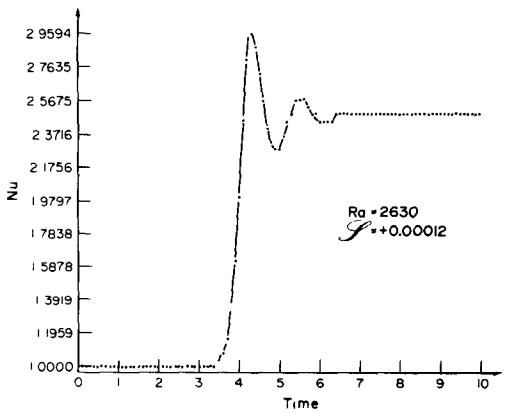

FIG. 6. Time variation of the Nusselt number ($0 \leqslant t \leqslant 10$); $Ra = 2630$; $\mathscr{S} = +1.2 \times 10^{-4}$.

constant for $t > 6.2$, but when the scale is amplified (Fig. 7; $t > 10$) very regular oscillations are observed;

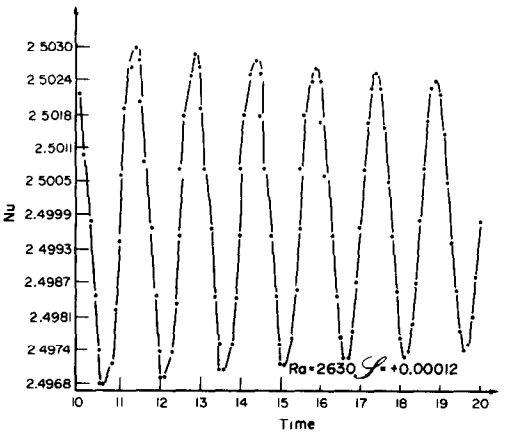

FIG. 7. Time variation of the Nusselt number ($10 \leqslant t \leqslant 20$); $Ra = 2630$; $\mathscr{S} = +1.2 \times 10^{-4}$.

moreover, the amplitude decreases slowly with time. $\mathbf{T}_{Nu}$ is now 1.5 in reduced units.

(f) *Results at* $Ra = 2630$ *and different* $\mathscr{S}$

The following runs were made

1. $\mathscr{S} = 0$ — usual Bénard problem.
2. $\mathscr{S} = +1.2 \times 10^{-4}$
3. $\mathscr{S} = -1.2 \times 10^{-4}$
4. $\mathscr{S} = +5 \times 10^{-4}$
5. $\mathscr{S} = -5 \times 10^{-4}$

   far from the neutral stability curve.
6. $\mathscr{S} = +10^{-2}$
7. $\mathscr{S} = -10^{-2}$
8. $\mathscr{S} = -5 \times 10^{-2}$ → close to the neutral stability curve.
9. $\mathscr{S} = -6 \times 10^{-2}$ → below the neutral stability curve.

In run 1, no oscillations are seen. In runs 2–7, we are far from the neutral stability curve. Oscillations are observed both for positive and negative Soret numbers. The period is absolutely not predicted by the linear theory and in the six runs is always equal to 1.5 reduced units and thus does not depend on the Soret number. On the contrary near the neutral stability curve the period is given by $\mathbf{T} \div 1/(|\mathscr{S}|)^{\frac{1}{2}} (\mathscr{S} < 0)$ according to the linear stability theory. However, the amplitude is influenced by the Soret number. We measured the greatest value of the amplitude after time $t = 10$. The situation is summarized in Table 3. We see that the amplitude is roughly proportional to $|\mathscr{S}|$.

Table 3

$\mathscr{S}$	$\mathbf{T}_{Nu}$	Maximum amplitude in Nu of the oscillations for $t > 10$
0	0	0
$+1.2 \times 10^{-4}$	1.5	0.0061
-1.2×10^{-4}	1.5	0.0060
$+5 \times 10^{-4}$	1.5	0.0251
-5×10^{-4}	1.5	0.0256
$+10^{-2}$	1.5	0.4959
-10^{-2}	1.5	0.5381

In run 8, we are "not too far" from the neutral stability curve (the Soret number at which $Ra^{crit}_{(over)} = 2630$ is -5.4×10^{-2}, whereas for $\mathscr{S} = -5 \cdot 10^{-2}$ we find $Ra^{crit}_{(over)} = 2483$). Integration was performed only for $t \leqslant 20$. We do not possess the new state, but for $t \leqslant 20$, the behaviour is completely identical to Fig. 4: instability arises as oscillations of increasing amplitude, with a period equal to $T_{Nu} = 1.26$ or $T_{\psi} = 2.52$. The period deduced from equation (11) is 2.55, thus in complete agreement with our observation. In run 9, we are below the critical point. The initial perturbation decreases with oscillations, in accordance with the overstability of the system for $\mathscr{S} < 0$. The behaviour of Nu is shown on Fig. 8. The Nusselt number reaches

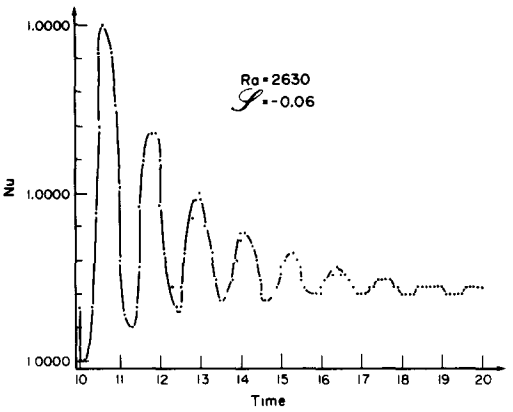

FIG. 8. Decay of the initial perturbation of the Nusselt number; $Ra = 2630$; $\mathscr{S} = -10^{-2}$.

the value 1.000000 by oscillations of decreasing amplitude.

(g) *Discussion of the results of Section* 3

The results that we have obtained in this paragraph could be summarized as follows:

(i) The results of the linear stability theory are recovered in these nonlinear computer experiments provided that the initial perturbation is small and that the Rayleigh number is close to the critical Rayleigh number. Both the "principle of exchange of stability" and "overstability" are observed in their particular range of validity: above (below) the critical point oscillations of increasing (decreasing) amplitude for $\mathscr{S} < 0$, but monotonous increase (decrease) in Nu for $\mathscr{S} > 0$. When oscillations are present their period is correctly predicted by the linear theory.

(ii) Far from the critical point, transient oscillations with more than one frequency are observed. For a sufficiently long time, the system reaches a final steady state, and the mean value of the Nusselt number is exactly the same as for the usual Bénard problem. Figure 9 shows the differences in Schmidt–Milverton plots between a pure liquid and a liquid mixture with a negative Soret coefficient ($\mathscr{S} < 0 \Rightarrow D'/D < 0$). These differences, as well as the experimental observations, were already discussed elsewhere [9, 15], but let us recall that very regular oscillations were observed in

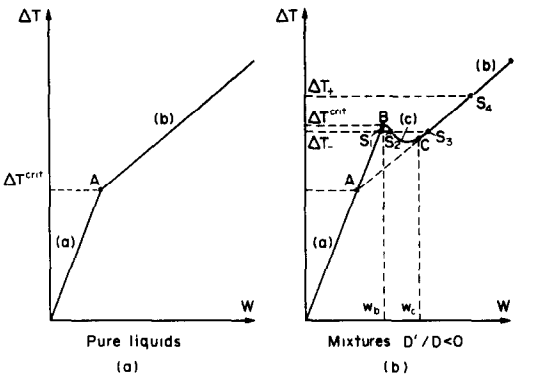

FIG. 9. Schmidt–Milverton plots for pure liquids (a) and mixtures with negative Soret coefficients (b). W is the heat power supplied to the Bénard apparatus.

the part of the curve with a negative slope [part (c)], i.e. below the critical temperature gradient. Far above the critical temperature gradient, e.g. $\Delta T = \Delta T_+$, there is only one state, whatever the initial conditions are, namely point S_4, and this state is probably a steady state. Starting from the state of rest, Hurle and Jakeman [16, 17] have shown experimentally that transient oscillations are observed when the heating power is increased, provided that the Rayleigh number is prevented to drop, and that finally the system reaches a final steady state. This is in fact exactly what we have observed and described in Sections 3(b) and (c). Finally, far from the critical point, the period of oscillations cannot be predicted by the linear theory, but, at a given Rayleigh number, their amplitude, is proportional to $|\mathscr{S}|$.

(iii) Below the critical point, say $\Delta T = \Delta T_-$, three states are possible, namely S_1, S_2 and S_3. S_1 is the state of rest and S_2 and S_3 convective states below the critical point ΔT^{crit}. The very nice oscillations reported previously [9] were observed below ΔT^{crit} but with a heating power W close to the critical heating power. W_b: the state S_2 is *probably* a finite amplitude oscillatory state. At a given Rayleigh number below Ra^{crit}, the state reached by the system will depend on the initial conditions. This will be examined in more detail in the next paragraph.

4. AN HYSTERESIS LOOP

Analytical calculations, related to a severe truncated development using only five coefficients [14] show the existence of stable steady convective states below the critical point and allow the description of an hysteresis loop in the Nusselt–Rayleigh plane. With this minimal representation for the velocity, temperature and concentration field, analytical calculations were made in order to find all the possible steady states. We have shown that two stable steady states were indeed possible below the critical point: the state of rest (say S_1 on Fig. 9, part b) and a convective steady state (interpreted as the state S_3 on Fig. 9). In order to reach this state S_3, special initial conditions must be specified,

namely initial conditions corresponding to a convective state, say S_4.

Of course, as already stated, we have to attach a physical meaning to numerical results which do not change in any significant way when the truncation level in the Fourier representation is increased. Numerical calculations, involving 16 coefficients ($P = Q = 2$) will not be reproduced here, because they produce numerical results identical to those obtained analytically, using the severe truncated development with only five coefficients. The particular good agreement between the results obtained with five and with 16 Fourier coefficients, is due to the fact that among the 16 coefficients, those with $(p+q)$ odd are not amplified. Moreover, among the remaining eight coefficients which are amplified, three are always much smaller than the five coefficients considered in the truncated expansion.

The numerical experiments that we have performed (with $P = Q = 4$) are summarized in Table 4.

Table 4, the mean value of the Nusselt number being 1.545. Thus the existence of an hysteresis loop is firmly established and is by no means linked to the number of Fourier coefficient, i.e. to a too small representation. The situation is summarized on Fig. 10.

5. COMPARISON WITH EXPERIMENTS

First of all, we would like to emphasize that a complete experimental study of the action of the Soret effect on natural convection is missing. We have no indication on the flow patterns in the nonlinear region, far from the critical point, and even, we do not possess the flow patterns near the critical point. The only experimental data available today are Schmidt–Milverton plots [3–5, 9, 16, 18, 19]. The aim of these experiments was to verify the variation of the critical Rayleigh number and to compare with the *linear* theory but by no means to know the flow structure. There is even

Table 4. Hysteresis loop with 56 Fourier coefficients ($\mathscr{S} = -10^{-2}$; $Ra^{crit}_{over} = 1028.35$)

Run No.	Ra	Initial state ($t = 0$)	Mean value of Nu during oscillations
1	$Ra^{crit} + 1000 = 2028.35$	Rest	2.70
2	1800	Run (1) at $t = 10$; $Nu(0) = 2.52$	2.55
3	1800	Rest	2.55
4	1500	Run (1) at $t = 10$	2.31
5	1200	Run (1) at $t = 10$	1.97
6	1200	Rest	1.98
7	1100	Run (1) at $t = 10$	1.85
8	$Ra^{crit} = 1028.35$	Run (1) at $t = 30$	1.73
9	1000	Run (5) at $t = 30$	1.71
10	$Ra^{crit} - 50 = 978.35$	Run (1) at $t = 30$	1.67
11	$Ra^{crit} - 100 = 928.35$	Run (1) at $t = 30$	1.55
12	913.85	Run (1) at $t = 10$	1.00

Let us now comment on some runs. Runs (2) and (3) show that, beyond the critical point, there is only one state corresponding to $Nu \simeq 2.55$, starting with the state of rest (run 3), or with a convective state. In col. 3 of Table 4, "Rest" means "At $t = 0$ all the Fourier coefficients are equal to zero except the initial perturbation given by $|B_{p,q}| = 10^{-6}$", whereas "Run (a) at $t = r$" means "At $t = 0$, all the Fourier coefficients are equal to the values obtained in run number (a) at time $t = r$". In run 9, we are below the critical Rayleigh number, and we know from the linear theory that if we start with the state of rest, slightly perturbed, the initial perturbation dies out and that the Nusselt number reaches the final value 1, with oscillations of decreasing amplitude (for the general behaviour see Fig. 8). However, if we start with an initial convective state, even below the critical point, the system does not return to the state of rest and the Nusselt number reaches a final mean value of 1.71. The same experiments are repeated in runs 10 and 11. From runs (11) and (12) we deduce that the Rayleigh number at which finite amplitude instability may exist is $913 < Ra_{f_a} < 928$, thus a larger value than that obtained with 16 or five coefficients. Nevertheless the hysteresis loop is still present. A supplementary run with 120 coefficients at $Ra = 928.35$ shows the same behaviour as run 11 of no information on the size of the convective cells compared with the case of a pure liquid. We would like to remember that the linear theory predicts that for

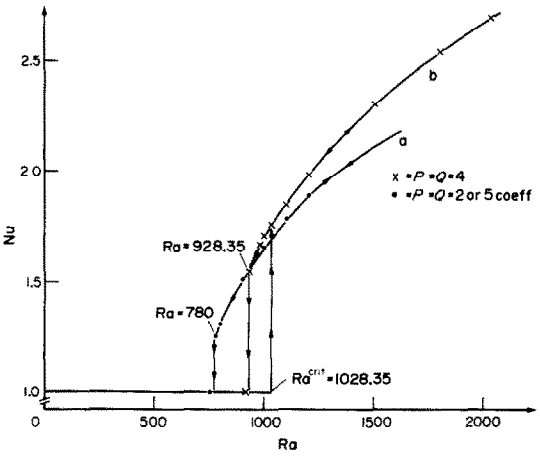

FIG. 10. Hysteresis loop in the Nusselt Rayleigh plane.

$\mathscr{S} > 0$, $k^{crit} \to 0$ or $\lambda^{crit} \to \infty$, where λ^{crit} is the critical wavelength linked to the size of the convective cells. In some sense, there would be only one convection cell for $\mathscr{S} > 0$, occupying the whole Soret apparatus and

this unique convection cell has no appreciable effect on the total heat transfer. This would in some sense explain why Schmidt–Milverton plots at $\mathscr{S} > 0$ show the same behaviour as for a pure liquid. Recently Sparasci and Tyrell [20] have obtained an experimental evidence for the existence of a critical limit for the onset of very slow convective motion at $\mathscr{S} > 0$, far below that associated with the normal Bénard motion. They used an optical system instead of simply measuring an increased heat flow.

The linear theory shows that, in some cases, overstability prevails at the critical point. As a consequence, the above mentioned researches have tried to detect oscillations near the critical point, at least in the temperature field, by looking at the response of a temperature probe (thermocouple, NTC resistor ...) fixed in a given position in the liquid layer. There still exists a controversy concerning the origin of the observed oscillations [17, 15]. Nevertheless we believe that the observed oscillations are really induced by thermal diffusion and our recent paper [9] shows qualitative agreement between experiments and theory as far as oscillations near the critical point are concerned. When the heating power is raised in Schmidt–Milverton plots, the thermocouple response becomes more irregular and finally oscillations seem to disappear (see e.g. Fig. 2, part C and D of [9]). This could be linked to the transient nature of the oscillations reported in this paper. Referring once more to Fig. 9, if the state S_4 is really a steady state and if overstability prevails at the critical point B it is quite natural to observe transient oscillations (both in laboratory experiments and in numerical experiments) during the evolution of the system from the state of rest to the convection steady state S_4. On the other hand, we were not able to reproduce in our numerical experiments sustained oscillations above the critical point. Let us recall that stable regular oscillations were only observed below the critical point (state S_2, Fig. 9) and that the experiment is conducted such that, being initially at the critical point B, one can evolve to the same Rayleigh number (ΔT_-) by two ways: by lowering the heat power or by increasing the heat power, and thus one can reach state S_1 or S_2 exactly as we like. On the contrary, in numerical experiments, the only parameter that we can vary is the Rayleigh number, and below the critical Rayleigh number the state reached by the system (S_1, S_2 or S_3) depends on the initial conditions, in some sense, depends on a certain preparation of the system. We were not able to prepare initially the system such as to reproduce the state S_2. It seems indeed difficult to find and to prescribe to all the Fourier coefficients the correct initial values such that each Fourier coefficient begins to oscillate with time.

The interpretation of the hysteresis loop described by our computer experiments is much more easy. In fact if the Rayleigh number is taken in numerical experiments as the *independent variable*, instead of the dependent variable as usually done in Schmidt–Milverton plots, the part of the curve in Fig. 9 with a negative slope (part C) cannot be reproduced by computer experiments, but only parts (a) and (b). Starting with the state of rest and, by increasing Ra, part (a) of the curve is retraced. If $Ra > Ra^{crit}$ ($\Delta T > \Delta T^{crit}$, e.g. $\Delta T = \Delta T_+$) there is a sudden jump to part (b) e.g. point S_4, corresponding to an increase in the Nusselt number. Now by decreasing Ra, part (b) of the curve is retraced and even below Ra^{crit}, stable convective states are possible. At point C, if we further decrease Ra, there is a new jump back to curve (a) corresponding to $Nu = 1$ (state of rest). This is in fact what is described on Fig. 10. A more qualitative comparison can be made. Referring to Fig. 10 of this paper we find

$$\frac{Ra^{crit}}{Ra_{min}} \simeq \frac{1028.35}{915} \simeq 1.123. \tag{14}$$

From Schmidt–Milverton plots on the system water–isopropanol (Fig. 3 of [9]) the ratio of the two temperature gradients at which the system leaves the state of rest by increasing the heat power, or returns back to the state of rest by decreasing the heat power, i.e. the ratio of the two ΔT's corresponding to point A and point C of Fig. 3 of [9], is 5.45°C/4.75°C $\simeq$ 1.147. Comparison of this result with (14) shows that the order of magnitude of the hysteresis loop is preserved, even if in equation (14) the numerical values of the dimensionless parameters (Pr, Sc, ...) are not exactly those corresponding to the experimental situation.

Finally, we believe, in order to make further progress in this problem, that a complete experimental study is needed, together with the solution for *rigid* boundaries. However, this second part is in progress, using finite differences.

Acknowledgement—We are deeply indebted to Professors I. Prigogine, P. Glansdorff and G. Nicolis whose continuous interest and stimulating comments were indispensible for the realization of this work. One of us (G.C.) wishes to thank the "Institut pour l'Encouragement de la Recherche Scientifique dans l'Industrie et l'Agriculture" (I.R.S.I.A., Brussels) for a grant.

REFERENCES

1. S. R. de Groot and P. Mazur, *Non Equilibrium Thermodynamics*. North Holland, Amsterdam (1962).
2. M. G. Velarde and R. S. Schechter, Thermal diffusion and convective stability (III): a critical survey of Soret coefficients measurements, *Chem. Phys. Lett.* **12**, 312 (1971).
3. J. C. Legros, D. Rasse and G. Thomas, Convection and thermal diffusion in a solution heated from below, *Chem. Phys. Lett.* **4**, 632 (1970).
4. J. C. Legros, W. A. Van Hook and G. Thomaes, Convection and thermal diffusion in a solution heated from below, *Chem. Phys. Lett.* **4**, 696 (1968).
5. J. C. Legros, W. A. Van Hook and G. Thomaes, (1968b), Convection and thermal diffusion in a solution heated from below, II: the system $CHBR_2 \cdot CHBR_2$–$CHCL_2 \cdot CHCl_2$, *Chem. Phys. Lett.* **2**, 249 (1968).
6. D. R. Caldwell, Measurements of negative thermal diffusion coefficients observing onset of thermohaline convection, *J. Phys. Chem.* **77**, 2004 (1973).
7. R. S. Schechter, M. G. Velarde and J. K. Platten, The two-component Bénard problem, *Adv. Chem. Phys.* **26**, 265 (1974).
8. J. K. Platten, Le problème de Bénard dans les mélanges:

cas des surfaces libres, *Bull. Acad. R. Belg. Cl. Sci.* **57**, 669 (1971).
9. J. K. Platten and G. Chavepeyer, Oscillatory motion in Bénard cell due to the Soret effect, *J. Fluid Mech.* **60**(2), 305 (1973).
10. G. Veronis, A note on the use of a digital computer for doing tedious algebra and programming, *Comm. ACM*, **8**, 205 (1965).
11. G. Veronis, Large-amplitude Bénard convection, *J. Fluid Mech.* **26**(1), 49 (1966).
12. G. Veronis, Motions at subcritical values of the Rayleigh number in a rotating fluid, *J. Fluid Mech.* **24**, 545 (1966).
13. T. D. Foster, The effect of initial conditions and lateral boundaries on convection, *J. Fluid Mech.* **37**, 81 (1969).
14. J. K. Platten and G. Chavepeyer, An hysteresis loop in the two component Bénard problem, *Int. J. Heat Mass Transfer* **18**, 1071 (1975).
15. J. K. Platten, G. Chavepeyer and J. Tellier, Finite amplitude oscillatory motions in the two component Bénard problem, *Phys. Lett.* **44A**, 479 (1973).
16. D. T. J. Hurle and E. Jakeman, Soret-driven thermosolutal convection, *J. Fluid Mech.* **47**, 667 (1971).
17. D. T. J. Hurle and E. Jakeman, Natural oscillations in heated fluid layers, *Phys. Lett* **43A**, 127 (1973).
18. D. R. Caldwell, Experimental studies on the onset of thermohaline convection, *J. Fluid Mech.* **64**, 347 (1974).
19. D. R. Caldwell, Non-linear effects in a Rayleigh–Bénard experiment, *J. Fluid Mech.* **42**, 161 (1970).
20. A. Sparasci and J. V. Tyrell, Thermal diffusion and convective stability: experimental study of the carbon tetrachloride–chlorobenzene system, *J. Chem. Soc. Faraday Trans.* **I**, **71**, 42 (1975).
21. G. Chavepeyer, Influence de l'Effet Soret sur la convection libre, Ph.D. Thesis, University of Mons (1974).

CONVECTION BIDIMENSIONNELLE NON LINEAIRE DE BENARD AVEC EFFET SORET: FRONTIERES LIBRES

Résumé—On décrit une analyse numérique de la convection d'amplitude finie dans un fluide à deux composants, en prenant en compte la diffusion thermique. Le problème considéré est équivalent au cas de la convection thermohaline avec un terme additionnel dans l'équation de diffusion, pour l'effet Soret. On intègre numériquement les équations non linéaires avec des conditions de frontière libre. Près de la courbe de stabilité neutre, les résultats de la théorie linéaire de la stabilité sont retrouvés pour les petites perturbations, mais on s'intéresse principalement aux amplitudes finies. Des résultats expérimentaux, récemment publiés, semblent montrer que des phénomènes nouveaux sont causées par l'effet Soret: essentiellement une boucle d'hystérésis avait été trouvée dans les diagrammes Schmidt–Milverton et des oscillations avaient été signalées lorsque le système binaire est chauffé par le bas. Cette étude tente de décrire théoriquement les faits expérimentaux. Durant l'intégration numérique des équations non linéaires, nous avons trouvé dans de nombreux cas des oscillations transitoires du nombre de Nusselt. Ces oscillations sont induites par l'effet Soret et la fréquence, ou l'amplitude, peut être reliée au coefficient de diffusion thermique. On révèle l'existence d'une convection à l'amplitude finie au dessous du nombre de Rayleigh critique (instabilités sous-critiques) et qu'une boucle d'hystérésis peut être décrite dans le plan des nombres de Nusselt et de Rayleigh.

NICHT-LINEARE, ZWEIDIMENSIONALE BENARD-KONVEKTION MIT SORET-EFFEKT: FREIE GRENZEN

Zusammenfassung—Diese Arbeit beschreibt eine numerische Analyse der Konvektion endlicher Amplitude in einem Zweikomponentenfluid unter Berücksichtigung der Thermodiffusion. Das vorliegende Problem entspricht dem Fall der thermohalinen Konvektion, wobei in der Diffusionsgleichung ein zusätzlicher Therm für den Soret-Effekt eingeführt werden muß. Die nicht-linearen Gleichungen mit freien Randbedingungen werden numerisch gelöst. In der Nähe der neutralen Stabilitätskurve wurden, wie zu erwarten war, die Ergebnisse der linearen Stabilitätstheorie für kleine Störungen bestätigt; das Hauptaugenmerk dieser Arbeit liegt jedoch auf der Konvektion endlicher Amplitude. Kürzlich veröffentlichte Versuchsergebnisse scheinen neue, durch den Soret-Effekt hervorgerufene physikalische Phänomene anzudeuten: vor allem wurde in den Schmidt–Milverton-Darstellungen eine Hysteresisschleife entdeckt und es wurde auch über Oszillationen in von unten beheizten Zweikomponentensystemen berichtet. Die vorliegende Arbeit versucht, die experimentellen Befunde theoretisch zu beschreiben. Bei der numerischen Lösung der nicht-linearen Gleichungen fanden wir in vielen Fällen Übergangsschwingungen in der Nusselt–Zahl. Diese Schwingungen werden durch den Soret-Effekt hervorgerufen und die Frequenz bzw. die Amplitude kann mit dem Thermodiffusionskoeffizienten in Verbindung gebracht werden. Es wird außerdem ein Nachweis der Konvektion endlicher Amplitude bei subkritischen Rayleigh–Zahlen (subkritische Instabilitäten) gegeben; damit kann eine Hysteresisschleife im Nusselt–Rayleigh-Diagramm beschrieben werden.

ДВУХМЕРНАЯ КОНВЕКЦИЯ БЕНАРА С УЧЕТОМ ЭФФЕКТА СОРЕ В НЕЛИНЕЙНОМ ПРИБЛИЖЕНИИ. СВОБОДНЫЕ ГРАНИЦЫ

Аннотация — Приводятся численные результаты по конвекции конечной амплитуды в двухкомпонентной жидкости с учетом термодиффузии. Данная задача аналогична задаче для случая термохалинной конвекции, только в уравнение диффузии добавлен член, учитывающий эффект Соре. Нелинейные уравнения со свободными граничными условиями интегрировались численно. Вблизи кривой нейтральной устойчивости результаты линейной теории справедливы для случая небольших возмущений, однако, основное внимание уделено исследованию конвекции конечной амплитуды. Последние опубликованные экспериментальные данные показывают, что эффект Соре вызывает новые физические явления: в частности, на графиках Шмидта-Мильвертона обнаружена петля гистерезиса, а также колебательная неустойчивость конвективного движения при нагреве двухкомпонентной системы снизу. Данная статья является попыткой теоретического описания экспериментальных данных. При численном интегрировании нелинейных уравнений во многих случаях наблюдались изменения во времени числа Нуссельта. Эти изменения могут быть связаны с коэффициентом термодиффузии. Приводятся также данные о конвекции конечной амплитуды для числа Релея, меньше критического (подкритическая неустойчивость), и, таким образом, петлю гистерезиса можно описать с помощью чисел Нуссельта и Релея.